Synthesis and Properties of Polyimide Ionomers Containing 1*H*-1,2,4-Triazole Groups

Jumpei Saito, Kenji Miyatake, and Masahiro Watanabe*

Clean Energy Research Center, University of Yamanashi, 4 Takeda, Kofu, Yamanashi 400-8510, Japan

Received December 16, 2007; Revised Manuscript Received January 18, 2008

ABSTRACT: A series of sulfonated polyimide copolymers containing 1*H*-1,2,4-triazole groups in the main chains were synthesized as proton-conducting membranes for fuel cell applications. Polycondensation of triazole-containing dianiline, acid-functionalized benzidine, and naphthalenetetracarboxylic dianhydride gave the title polyimide ionomers. The ionomers were high molecular weight (M_w > 100 kDa, M_n > 20 kDa) to give tough and flexible membranes by solution casting. The ion exchange capacity (IEC) of the membranes ranged from 1.10 to 2.68 mequiv/g as confirmed by ^{1}H NMR analyses and titration. Comparison with the other polyimide ionomer membranes revealed that introducing triazole groups caused better thermal stability (decomposition temperature of ca. 200 °C), comparable hydrolytic and oxidative stability, and better mechanical properties. Although NH groups did not function as ion exchange sites, the triazole-containing membranes showed slightly higher proton conductivity. The highest proton conductivity (0.3 S/cm at 88% RH) was obtained for the high IEC (2.68 mequiv/g) ionomer membrane. The ionomer membranes showed low hydrogen and oxygen permeability under dry and wet conditions.

Introduction

Proton-conducting polymers are in great demand as membranes in polymer electrolyte membrane fuel cells (PEMFCs).[1–3] The state-of-the-art membrane materials are perfluorosulfonic acid polymers such as Nafion (Du Pont) which consist of polytetrafluoroethylene main chains and sulfoperfluoroalkyl ether side chains. In terms of high-temperature capability, environmental friendliness (recyclability), and production cost, nonfluorinated alternative materials have been under development.[4] Aromatic ionomers are one of the promising candidates since they are thermally stable, easy to modify chemically, and inexpensive.[5] Although a number of aromatic ionomers have been proposed in the past decade or two, stability and proton conductivity remain issues and must be improved.[6]

We have investigated the molecular structures of sulfonated polyimide ionomers and found out that aromatic/aliphatic polyimide (SPI-5) ionomers containing alkylene segments both in the main and the side chains are thermally, hydrolytically, oxidatively, and mechanically stable.[7,8] The membranes therefrom were durable for 5000 h in a hydrogen/air fuel cell without distinct degradation.[9] However, the proton conductivity at low humidity is insufficient for the practical applications and needs to be improved.

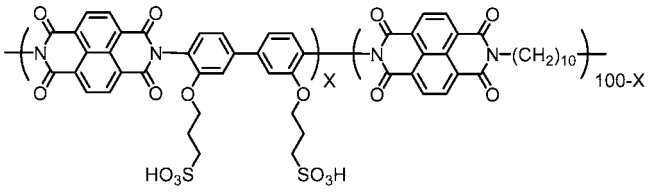

SPI-5

Imidazole compounds, as replacements for water, are known to facilitate proton transport in polymer electrolyte membranes under low humidity or anhydrous conditions.[10–12] Phosphoric acid doped poly(benzimidazole) shows high proton conductivity under high temperature and anhydrous conditions.[13,14] However, high doping levels are generally required and the conductivity drops at the loss (dedoping) of acid dopants especially when exposed to water.[15] Imidazole and imidazole-containing polymers (without acid dopants) have been also investigated.[16] Recently, triazoles have been investigated as a better proton conduction medium since triazoles have more acidic NH groups (pK_a1 = 1.17 for 1*H*-1,2,3-triazole and pK_a1 = 2.39 for 1*H*-1,2,4-triazole) than that of imidazole (pK_a1 = 7.18) and thus should be better protonic carriers.[17] Poly(acrylonitrile) blends with triazole[18] and poly(vinyltriazole)[19,20] have been reported to show enhanced proton conductivity. To the best of our knowledge, systematic study on the effect of triazole groups on the properties of aromatic ionomers has not yet been done.

The objective of the present study is to look into the effect of triazole groups on the properties of sulfonated polyimide ionomers. A series of new polyimide ionomers containing 1*H*-1,2,4-triazole groups in the main chains were synthesized, in which ion exchange capacity (IEC) was varied by changing the copolymer composition. Their properties such as thermal and chemical stability, mechanical strength, water uptake behavior, proton conductivity, and gas permeability have been investigated in detail and compared with our previous polyimide ionomers with no triazole groups (SPI-5).

Experimental Section

Materials. 1,4,5,8-Naphthalenetetracarboxylic dianhydride (TCND) (Aldrich) was used as received. 3,3′-Bis(sulfopropoxy)-4,4′-diaminobiphenyl (BSPA) was synthesized from 3,3′-dihydroxybenzidine (98%, TCI) and 1,3-propanesultone (Kanto Chemicals) according to the literature.[8] This monomer was characterized by ^{1}H NMR spectrum and stored in the dark. Triethylamine (TEA) (Aldrich) and benzoic acid (Kanto Chemicals) were used as received. *m*-Cresol was dried over molecular sieves 3A prior to use. Other chemicals were of commercially available grade and used as received.

3,5-Bis(4-aminophenyl)-1*H*-1,2,4-triazole (APTAZ). APTAZ was synthesized from 4-aminobenzohydrazide (ABH) (98%, TCI) and 4-aminobenzonitrile (ABN) (98%, TCI) according to the literature.[21] This monomer was characterized by liquid chromatography/mass spectroscopy (LC/MS) and ^{1}H NMR spectrum. It was stored in the dark.

* To whom correspondence should be addressed. Tel.: 81-55-220-8620. Fax: 81-55-254-0371. E-mail: m-watanabe@yamanashi.ac.jp.

10.1021/ma7028055 CCC: $40.75
Published on Web 03/13/2008

Polymerization. A typical procedure for the copolymerization is as follows. BSPA (1 mmol), APTAZ (1 mmol), TEA (10.8 mmol), and 10 mL of *m*-cresol were placed in a four-neck round-bottomed flask equipped with a magnetic stirring bar and N_2 inlet. The mixture was stirred at 50 °C. After a clear solution was obtained, TCND (2 mmol) and benzoic acid (4 mmol) were added into the mixture. The mixture was then cooled to room temperature and stirred under a stream of N_2. The mixture was heated at 175 °C for 15 h and at 195 °C for 3 h. After the reaction, the mixture was poured dropwise into a large excess of acetone. The yellow fibrous precipitate was filtered, washed with acetone, and dried at 80 °C under reduced pressure for 12 h to obtain SPI-8(50).

Membrane Preparation. The ionomer SPI-8 (0.4 g) was dissolved in 12 mL of dimethyl sulfoxide (DMSO) and cast onto a flat glass plate. After drying at 60 °C, a crude membrane in salt form was immersed in ethanol containing 1 N HNO_3 for 12 h. The acidification procedure was repeated three times followed by washing with pure ethanol. After drying at 80 °C under reduced pressure for 12 h, the ionomer SPI-8 membrane in acid form was obtained with a thickness of 50 μm.

Measurement. ^{1}H (400 MHz) NMR spectra were recorded on a Bruker AVANCE 400S spectrometer with deuterated dimethyl sulfoxide (DMSO-d_6) as a solvent and tetramethylsilane (TMS) as an internal reference. LC/MS experiments were performed on a Shimadzu SPD-M10Avp (column: Shodex VP-ODS) and a Shimadzu LCMS-2010A. Molecular weight was measured with gel permeation chromatography (GPC) equipped with two Shodex KF-805 columns and a Jasco 805 UV detector (270 nm) with DMF containing 0.01 M LiBr as eluent. Molecular weight was calibrated with standard polystyrene samples. Ion exchange capacity (IEC) of the ionomer membranes was determined by ^{1}H NMR spectra and titration. In the titration method, a piece of ionomer membranes was equilibrated in large excess of 0.01 M NaCl aq for 15 h. The concentration of HCl released from the membrane sample was measured by titration with 0.01 N NaOH aq using phenolphthalein as an indicator.

Thermal Properties. Thermal analyses were performed via TG/DTA-MS with a Mac Science TG/DTA 2000 equipped with a Bruker MS 9600 mass spectrometer at a heating rate of 5 °C/min under argon.

Hydrolytic Stability. A small piece of membrane sample with a thickness of 50 μm was treated in water at 140 °C for 24 h. The stability was evaluated by changes in IEC, molecular weight, and weight of the test samples.

Oxidative Stability. A small piece of membrane sample with a thickness of 50 μm was soaked in Fenton's reagent (3% H_2O_2 containing 2 ppm $FeSO_4$) at 80 °C for 1 h. The stability was evaluated by changes in IEC, molecular weight, and weight of the test samples.

Mechanical Properties. Tensile testing was performed with a Shimadzu universal testing instrument Autograph AGS-J500N equipped with a chamber in which the temperature and the humidity were controlled by flowing humidified air with a Toshin Kogyo temperature control unit Bethel-3A. The membrane was equilibrated at the set temperature and humidity for at least 3 h before the measurement. Stress versus strain curves were obtained at 93% RH and 85 or 120 °C at a stretching speed of 10 mm/min for samples cut into a dumbbell shape (DIN-53504-S3, 35 mm × 6 mm (total) and 12 mm × 2 mm (test area)). Compression creep testing was performed with a Toyo-seiki compression creep testing machine equipped with a chamber and a Bel Japan humidified gas supplier RDT-129. For the compression creep measurement, membrane samples (25 mm wide, 70 mm long, and 50 μm thick) were set in the chamber where the temperature and the humidity were controlled by flowing humidified N_2. The membrane was equilibrated at the set temperature and humidity for at least 2 h before the measurement. The measurement was done at 80 or 120 °C and 60% RH with 42 kgf/cm^2 of loading for 15 h.

Water Uptake and Proton Conductivity. Water uptake and proton conductivity of the ionomer SPI-8 membranes were measured with a Bel Japan solid electrolyte analyzer system MSB-AD-V-FC equipped with a chamber, a magnetic suspension balance, and a four-point probe conductivity cell. For water uptake measurement, a membrane sample (40−60 mg) was set in a chamber and dried at 80 °C under vacuum for 3 h until constant weight as dry material was obtained. The membrane was then equilibrated with N_2 gas at given temperature and humidity for at least 1 h before the gravimetry was done.

For the proton conductivity measurement, the membrane sample (1.0 cm wide, 3.0 cm long, and 50 μm thick) were set in the chamber where the temperature and the humidity were controlled by flowing humidified N_2. The membrane was then equilibrated with N_2 gas at the set temperature and humidity for at least 1 h before the measurement. The sample was contacted with two gold wire outer current-carrying electrodes and two gold wire inner potential-detecting electrodes. Impedance measurements were made using a Solartron 1255B frequency response analyzer and Solartron SI 1287 potentiostat. The instrument was used in potentiostatic mode with an ac amplitude of 300 mV with the frequency range from 10 to 100 000 Hz.

Gas Permeability. Hydrogen and oxygen permeability of the ionomer membranes was measured with a GTR-Tech 20XFYC gas permeation measurement apparatus equipped with a Yanaco G2700T gas chromatography. The gas chromatography contained a Porapak-Q column and a TCD detector. Argon and helium were used as a carrier gas for the measurement of hydrogen and oxygen, respectively. A membrane sample (30 mm in diameter and 50 μm thick) was set in a cell that had a gas inlet and outlet on both sides of the membrane. On one side of the membrane, dry or humidified test gas (hydrogen or oxygen) was supplied at a flow rate of 50 mL/min, while on the other side of the membrane, the same gas as the carrier used in the gas chromatograph (flow gas) was supplied at a flow rate of 20 mL/min. The flow gas was humidified under the same conditions as the test gas so as to keep the membrane's wetting uniform. Before each measurement was done, the membrane was equilibrated with the gases at the given temperature and humidity for at least 3 h. Then 3.7 mL of flow gas was sampled and subjected to the gas chromatography to quantify the test gas permeated through the membrane. The gas permeation rate, r (cm^3 (STD) cm^{-2} s^{-1}), and the gas permeation coefficient, Q (cm^3 (STD) cm cm^{-2} s^{-1} cmHg^{-1}), were calculated according to the following equations:

$$r = \frac{273}{T}\frac{1}{A}B\frac{1}{t}$$

$$Q = \frac{273}{T}\frac{1}{A}B\frac{1}{t}l\frac{1}{76 - P_{H_2O}}$$

where T (K) is the absolute temperature of the cell, A (cm^2) is the permeation area, B (cm^3) is the volume of test gas permeated through the membrane, t (s) is the sampling time, l (cm) is the thickness of the membrane, and P_{H_2O} (cmHg) is the water vapor pressure.

Results and Discussion

Synthesis and Characterization of Monomers and Ionomers. In order to prepare the sulfonated polyimides containing 1*H*-1,2,4-triazole groups in the main chains, 3,5-bis(4-aminophenyl)-1*H*-1,2,4-triazole (APTAZ) was synthesized by the condensation reaction of 4-aminobenzohydrazide (ABH) and 4-aminobenzonitrile (ABN) under basic conditions. After the reaction, the crude product was purified by crystallization from ethanol/water to give a pale yellow crystal of APTAZ in 27% yield. The purity of APTAZ was high enough for the polymerization reactions as confirmed by ^{1}H NMR and LC/MS analyses. The polycondensation reaction of TCND, BSPA and APTAZ was carried out in *m*-cresol in the presence of excess triethylamine (Scheme 1).

The feed monomer ratio ([BSPA]/[TCND]) was varied from 0.3 (X = 30) to 0.9 (X = 90) to obtain a series of SPI-8(X)

Scheme 1. Synthesis of Triazole-Containing Polyimide Ionomers SPI-8(*X*)

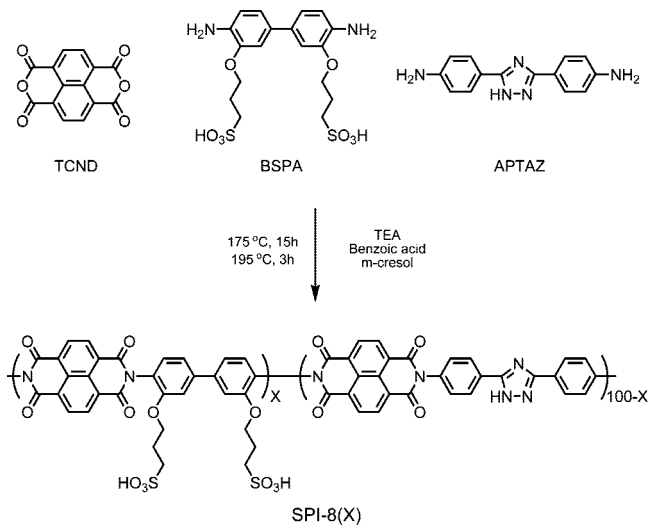

Table 1. Molecular Weight and Ion Exchange Capacity (IEC) of SPI-8(*X*) Membranes

polymer	M_n (kDa)	M_w (kDa)	M_w/M_n	IEC[a] (mequiv/g)	IEC[b] (mequiv/g)	IEC[c] (mequiv/g)
SPI-8(30)	27.1	109.6	4.0	1.10	1.17	1.00
SPI-8(50)	56.6	191.8	3.4	1.70	1.76	1.68
SPI-8(70)	111.9	295.0	2.6	2.22	2.22	2.17
SPI-8(80)	105.3	338.2	3.2	2.46	2.46	2.47
SPI-8(90)	120.2	323.8	2.7	2.68	2.70	2.69

[a] Calculated from the feed monomer ratio. [b] Obtained from the ^{1}H NMR spectra. [c] Obtained from the titration.

copolymers in which *X* represents molar percentage of BSPA. The calculated value of ion exchange capacity (IEC) of the SPI-8 ranges from 1.10 to 2.68 mequiv/g. All of the SPI-8 copolymers were obtained as a fiber by precipitation from acetone. The SPI-8 copolymers are soluble in polar aprotic solvents such as DMSO and NMP. GPC analyses revealed that the SPI-8 copolymers are high-molecular-weight (M_w > 100 kDa, M_n > 20 kDa) (Table 1). Molecular weight decreased with increasing the amount of triazole groups. It is because increased ionic content causes increased bulkiness of polymer chains and short retention time in GPC analyses. SPI-8 copolymers were characterized by ^{1}H NMR spectra. As a typical example, ^{1}H NMR spectrum of SPI-8(90) is shown in Figure 1. The peaks of aromatic and aliphatic protons could be well assigned to the supposed chemical structure. The IEC value (2.70 mequiv/g) obtained from the integration ratio of the peaks (f: i + i′) in Figure 1 is in good accordance with the calculated value (2.68 mequiv/g). The results confirm that the composition of SPI-8(90) copolymer corresponds to the feed monomer ratio. The NMR analyses confirmed that the other copolymers have similar IEC values to the calculated ones as summarized in Table 1.

Casting DMSO solutions of SPI-8 copolymers gave membranes with a thickness of ca. 50 μm. The obtained membranes were of brown color typical for polyimides with toughness and flexibility. The SPI-8 membranes were transparent when X = 70, 80, and 90, while a somewhat turbid membrane was obtained from SPI-8(30) due to its higher crystallinity. The higher crystallinity of SPI-8(30) with higher content of triazole groups (70 mol %) would be reasonable, taking the linear, rodlike structure of diphenylene triazole groups into account. IEC values obtained by titration of the SPI-8 membranes are in good accordance with the ones by calculation and NMR analyses. The results imply that all the sulfonic acid groups function well as ion exchange sites in the membrane while the NH groups in

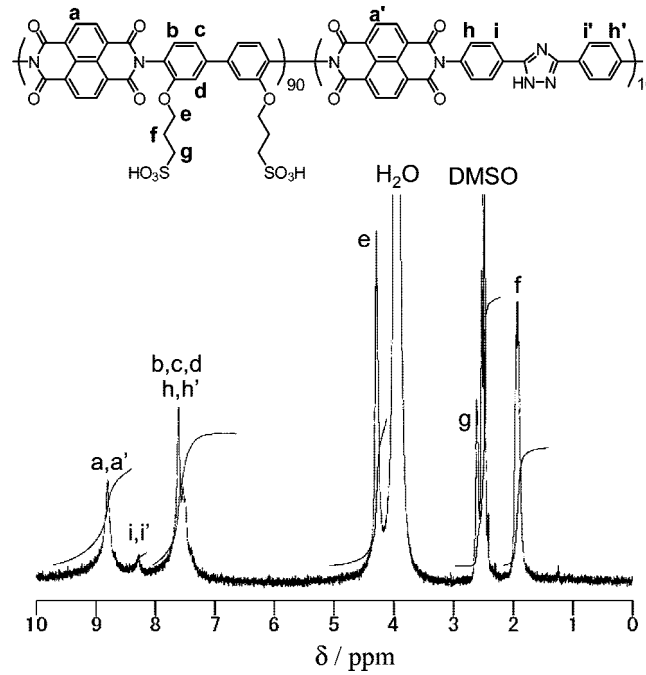

Figure 1. ^{1}H NMR spectrum of SPI-8(90) in DMSO-d6.

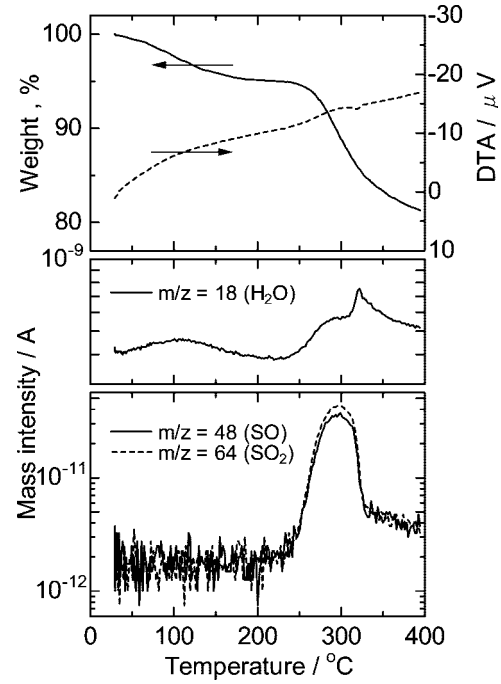

Figure 2. TG/DTA and MS curves of SPI-8(50) under dry Ar atmosphere.

triazole moieties do not. Dissociation of the NH groups would be significantly restricted as they are anchored in the polymer main chains and are in the vicinity of sulfonic acid groups as stronger acids.

Thermal, Hydrolytic, Oxidative, and Mechanical Stability of SPI-8 Membranes. Since ionomer membranes are subjected to heat, high-temperature water, oxidative environment, and substantial pressure under fuel cell operation, the SPI-8 copolymer membranes were tested in harsh and accelerated conditions. The thermal stability was first investigated by TG/DTA-MS analyses under dry Ar atmosphere. Typical TG/DTA-MS curves are shown in Figure 2 for SPI-8(50). In the TGA curve, two-step weight losses were observed from room

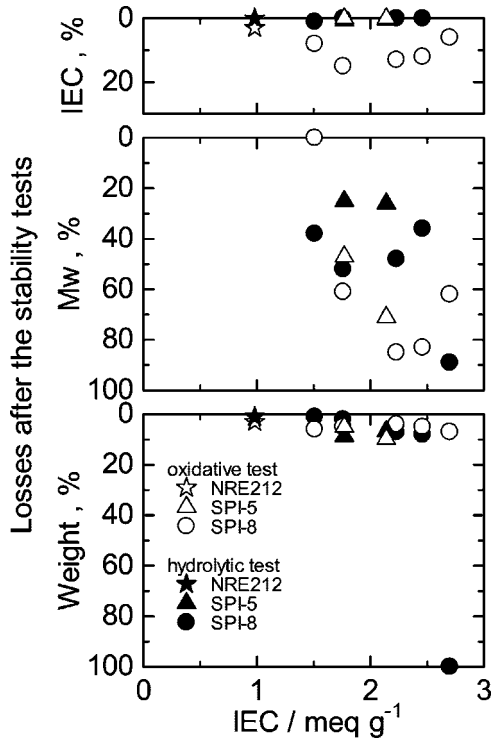

Figure 3. Hydrolytic and oxidative stability of SPI-5, SPI-8, and Nafion NRE212 membranes as a function of IEC.

temperature to 180 °C and above 200 °C. By combining TG with MS chromatograms, the first weight loss was assigned to the evaporation of hydrated water (H_2O = 18 *m/z*) and the second one was due to the decomposition of the ionomer (SO = 48, SO_2 = 64 *m/z*). The major fragment ions observed in the second weight loss were SO and SO_2, indicating that the thermal decomposition commenced by the degradation of sulfonic acid groups in the side chains. The onset decomposition temperature of SPI-8 membranes is about 50 °C higher than that of our previous polyimide SPI-5 membranes (the onset decomposition temperature of SPI-5 is 150 °C).[8] As has been suggested from the titration experiments, the NH groups of 1*H*-1,2,4-triazole groups are likely to have interaction with the sulfonic acid groups via hydrogen bonding which would be responsible for the higher decomposition temperature of SPI-8 compared to that of SPI-5. In the DTA curves, no glass transition was observed below the decomposition temperature for all the SPI-8 copolymers.

Under the wet conditions, hydrolytic and oxidative stability of the SPI-8 membranes were tested. In both experiments, changes in IEC, molecular weight, and weight of the membranes were plotted as a function of IEC in Figure 3. For comparison, the stability data are also given for the SPI-5 and Nafion NRE212 membranes (no molecular weight data are provided for Nafion NRE membrane since our GPC system is not available for nonaromatic polymers). In the hydrolytic stability tests (closed symbols), all SPI-8 membranes showed high stability without losing their IEC values. Although SPI-8(90) membrane with the highest IEC of 2.70 mequiv/g dissolved in water (100 wt % loss), the other membranes with lower IEC lost merely less than 10% of the weight. The loss in molecular weight was dependent on the IEC with a general trend of higher molecular weight loss for higher IEC membranes. The membranes became brittle when the molecular weight loss was higher than ca. 50%. In the postmortem NMR analyses, three minor peaks were observed at 6.90−7.10 ppm assignable to the naphthaleic moieties with ring-opened imide groups. These results suggest that the main chain degradation is caused by hydrolysis of imide groups (reverse polymerization). There are no noticeable differences observed in the hydrolytic stability between SPI-8 and SPI-5 series since they share the same hydrophilic copolymer component (3,3′-bis(sulfopropoxy)-4,4′-biphenylene groups).

Table 2. Mechanical Properties of SPI-5, SPI-8, and Nafion NRE212 Membranes at 93% RH

membrane	IEC (mequiv/g)	maximum stress (MPa) 85 °C	maximum stress (MPa) 120 °C	elongation at break (%) 85 °C	elongation at break (%) 120 °C	Young's modulus (GPa) 85 °C	Young's modulus (GPa) 120 °C
SPI-8(50)	1.76[a]	103	70	28	12	1.20	1.76
SPI-8(70)	2.22[a]	53	53	18	6	1.10	1.48
SPI-8(80)	2.46[a]	43	26	11	2	1.23	1.51
SPI-8(90)	2.70[a]	45	35	17	8	0.55	0.64
SPI-5(50)	1.82[a]	34	29	9	10	1.00	1.00
SPI-5(70)	2.31[a]	16	12	17	6	0.36	0.20
NRE212	0.98[b]	12	8	477	411	0.002	0.0009

[a] Obtained from the ^{1}H NMR spectra. [b] Data from the supplier (Du Pont).

The oxidative stability of SPI-8 membranes was evaluated in hot Fenton's reagent as an accelerated testing and is shown as open symbols in Figure 3. The loss in IEC in oxidative tests seemed independent of the IEC of SPI-8 membranes and was larger than that in hydrolytic tests. The weight and molecular weight losses in oxidative tests were almost comparable to those in hydrolytic tests. The three peaks discussed above were also observed for the samples after oxidative tests. Therefore, we conclude that the major degradation mode is the same for both in hydrolytic and oxidative tests involving imide ring opening while certain degree of side chain degradation occurs by oxidative attack of radical species ($HO^\bullet$ and $HOO^\bullet$). In these tests, our new SPI-8 membranes showed comparable hydrolytic and oxidative stability to SPI-5 membrane. Nafion NRE212 membrane was robust and showed only minor losses in IEC and weight under the same conditions.

Mechanical properties of the SPI-8 membranes were evaluated with tensile testing (in-plane direction) and compression creep testing (through-plane direction) under controlled temperature and humidity. The results of the tensile testing are summarized in Table 2.

The SPI-8 membranes exhibited better mechanical properties, higher maximum stress (>43 MPa at 85 °C and >26 MPa at 120 °C) and lower elongation at break (<28% at 85 °C and <12% at 120 °C), than those of Nafion NRE 212. The results indicate that the SPI-8 membranes have good dimensional stability at high temperature and humidity. Comparison between SPI-5 and SPI-8 membranes with comparable IEC value showed that the triazole-containing SPI-8 membranes are much more mechanically stable. For example, maximum stress of SPI-8(70) was more than 3 times (85 °C) and 4 times (120 °C) higher than that of SPI-5(70). SPI-8(50, 70, 80) membranes have very high Young's modulus (>1 GPa) at both temperatures. High mechanical strength would be attributable to the intermolecular interaction among triazole groups and sulfonic acid groups. Therefore, with increasing IEC (decreasing the amount of triazole groups), Young's modulus of the membranes became smaller. As discussed below, larger water uptake in higher IEC membranes is also responsible for the lowered Young's modulus. It should be noted that the SPI-8 membranes have higher Young's modulus at 120 °C than at 85 °C while increasing temperature had negative effect on the mechanical properties of SPI-5 and NRE212 membranes. It might be due to the annealing effect on the SPI-8 membranes.

Compressive creep deformation of SPI-8(80) and Nafion NRE212 membranes was plotted as a function of time in Figure 4. Both membranes showed small deformation within the first 1 h and negligible thereafter at 80 °C and 60% RH. Similar

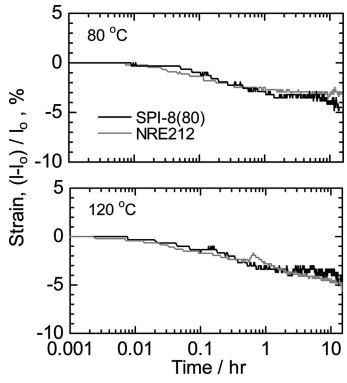

Figure 4. Time course of the compressive creep deformation of SPI-8(80) and Nafion NRE212 membranes at 80 and 120 °C and 60% RH.

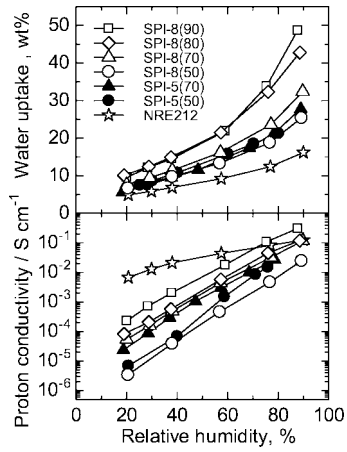

Figure 5. Humidity dependence of the water uptake and the proton conductivity of SPI-5, SPI-8, and Nafion NRE212 membranes at 80 °C.

results were obtained at higher temperature (120 °C). The creep deformation of SPI-8(80) membrane was 4−5% after 15 h, which was comparable to that of NRE212. The results seem in conflict with the tensile properties in Table 2. However, taking into account that polyimide ionomer membranes with pendant acid groups show anisotropic swelling behavior with much higher swelling degree in through-plane direction than in-plane direction by a factor of up to 10,[22] rather large deformation of SPI-8(80) in through-plane direction would be reasonable. Since very high load (42 kgf/cm^2) was applied to membranes in the creep deformation testing, the SPI-8 membranes are potentially applicable to fuel cells in which membrane electrode assembly is tightened with separators at a typical pressure of 10−15 kgf/cm^2.

Water Uptake and Proton Conductivity. Humidity dependence of the water uptake and proton conductivity was measured at 80 °C for a series of SPI-8 membranes with different IEC values and compared with that of SPI-5(70) and Nafion NRE212 (Figure 5). All the SPI membranes showed larger water uptake than that of NRE212 at all humidity conditions. Higher IEC membranes absorbed more water. This tendency was more pronounced at higher humidity. SPI-8(90) with the highest IEC showed the largest water uptake of 49% at 88% RH. SPI-8(70) showed slightly larger water uptake than that of SPI-5(70) despite of the former's lower IEC. Although the NH groups in triazoles do not function as ion exchange sites (see above), they could contribute to more hydrophilicity in SPI-8 membranes.

SPI-8(70, 80, 90) membranes with higher IEC than 2.22 mequiv/g showed comparable proton conductivity to that of

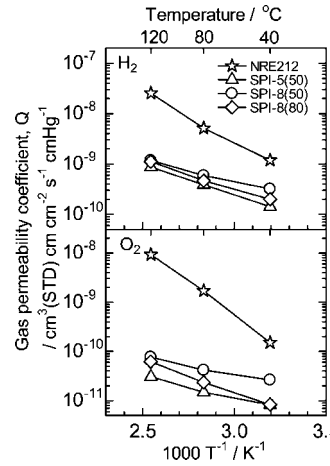

Figure 6. Temperature dependence of the dry hydrogen and oxygen permeability of SPI-5, SPI-8, and Nafion NRE212 membranes.

NRE212 at high humidity. However, the proton conductivity of SPI-8 membranes showed greater dependence on the humidity which resulted in more than 1 order of magnitude lower conductivity than that of NRE212 at 20% RH. Less dependence of the conductivity on humidity for the Nafion membrane is attributable to the well-developed and well-connected hydrophilic domains that are several nanometers in diameter and act as proton transporting channels. In contrast, nonfluorinated ionomer membranes are less likely to have such hydrophilic domains and thus lose much of the conductivity at low humidity.[23] This is also the case for SPI-8 membranes. The proton conductivity of the SPI-8(70) membrane was higher than that of SPI-5(70) at all humidities examined. Although the difference was not very distinctive, introducing triazole groups into polyimide ionomers was effective in improving the proton conductivity. However, the effect was not clearly observed for the lower IEC SPI-8(50) membrane compared to SPI-5(50). The best proton conductivity was obtained for SPI-8(90) membrane: 2×10^{-4} S/cm at 20% RH and 0.3 S/cm at 88% RH.

Gas Permeability. Temperature dependence of dry hydrogen and oxygen permeability coefficient (Q) of SPI-5(50), SPI-8(50, 80), and NRE212 membranes is shown in Figure 6. All the polyimide ionomer membranes were much less permeable to both gases than NRE212. The less permeability was more pronounced for oxygen than hydrogen, because NRE212 as perfluorinated polymers are more oxophilic than nonfluorinated polymers. Since log Q was almost linear to the reciprocal temperature, apparent activation energy of gas permeation was calculated from the slope to give $E_a(H_2) = 39$ and $E_a(O_2) = 53$ kJ/mol (NRE212), $E_a(H_2) = 17$ and $E_a(O_2) = 14$ kJ/mol (SPI-8(50)), and $E_a(H_2) = 22$ and $E_a(O_2) = 26$ kJ/mol (SPI-8(80)), respectively. Comparison between SPI-5(50) and SPI-8(50) revealed that the introducing triazole groups induced slight increase in gas permeability, especially oxygen, indicating heterocyclic triazole moieties could solubilize more oxygen. Higher IEC resulted in lower gas permeability since gases permeate mainly through hydrophobic domain of ionomer membrane.[24]

Humidity dependence of hydrogen and oxygen permeability coefficient (Q) of SPI-5(50), SPI-8(50, 80), and NRE212 membranes at 80 °C is shown in Figure 7. The gas permeability of polyimide ionomer membranes was significantly lower than that of NRE212 under any humidity conditions. Gas permeability increased with increasing the humidity due to the swelling of membranes. Unlike the dry conditions, SPI-8(50) showed the lowest gas permeability under the humidified conditions. The results could not be simply explained by the water uptake

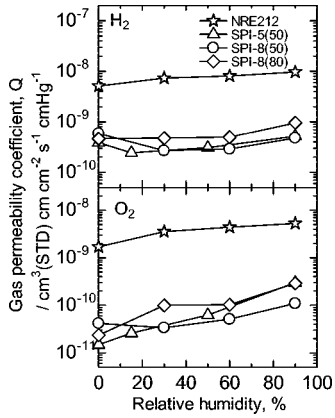

Figure 7. Humidity dependence of hydrogen and oxygen permeability of SPI-5, SPI-8, and Nafion NRE212 membranes at 80 °C.

behavior (Figure 5). Since SPI-8(50) was the only sample that showed reverse-volcano type dependence on the humidity for both of hydrogen and oxygen permeability, low swellability would be accountable for the lowest gas permeability.

Conclusions

We have synthesized a new series of polyimide ionomers containing 1*H*-1,2,4-triazole groups in the main chains and sulfonic acid groups in the side chains. The following important facts were obtained.

1. The triazole groups tethered in the sulfonated polyimide structure did not function as ion exchange sites probably due to the interaction with the sulfonic acid groups, possibly via hydrogen bonding.

2. Introducing triazole groups improved thermal decomposition temperature (by 50 °C) and mechanical stability (in-plane and through-plane directions), while it did not practically affect hydrolytic and oxidative stability of polyimide ionomer membranes.

3. Higher proton conductivity was obtained for triazole-containing polyimide ionomers than the non-triazole-containing equivalents due to the increased water uptake but not to the acidic nature of triazole groups.

4. Introducing triazole groups increased dry gas permeability; however, it had the opposite effect under humidified conditions.

These properties of triazole-containing polyimide ionomers seem promising for fuel cell applications, which are currently under investigation and will be reported elsewhere.

Acknowledgment. This work was partly supported by MEXT Japan through the fund for Leading Project "Next Generation Fuel Cells" and a Grant-in-Aid for Scientific Research (18750167).

References and Notes

(1) Appleby, A. J.; Foulkes, F. R. *Fuel Cell Handbook*; Van Nostrand Reinhold: New York, 1989.
(2) Carratte, L.; Friedlich, K. A.; Stimming, U. *Fuel Cells* **2001**, *1*, 5–39.
(3) Steele, B. C. H.; Heinzel, A. *Nature (London)* **2001**, *414*, 345–352.
(4) Miyatake, K.; Watanabe, M. *Electrochemistry (Tokyo, Jpn.)* **2005**, *73*, 12–19.
(5) Hickner, M. A.; Ghassemi, H.; Kim, Y. S.; Einsla, B. R.; McGrath, J. E. *Chem. Rev.* **2004**, *104*, 4587–4611.
(6) Borup, R.; Meyers, J.; Pivovar, B.; Kim, Y. S.; Mukundan, R.; Garland, N.; Myers, D.; Wilson, M.; Garzon, F.; Wood, D.; Zelenay, P.; More, K.; Stroh, K.; Zawodzinski, T.; Boncella, J.; McGrath, J. E.; Inaba, M.; Miyatake, K.; Hori, M.; Ota, K.; Ogumi, Z.; Miyata, S.; Nishikata, A.; Siroma, Z.; Uchimoto, Y.; Yasuda, K.; Kimijima, K.-i.; Iwashita, N. *Chem. Rev.* **2007**, *107*, 3904–3951.
(7) Asano, N.; Miyatake, K.; Watanabe, M. *Chem. Mater.* **2004**, *16*, 2841–2843.
(8) Asano, N.; Aoki, M.; Suzuki, S.; Miyatake, K.; Uchida, H.; Watanabe, M. *J. Am. Chem. Soc.* **2006**, *128*, 1762–1769.
(9) Aoki, M.; Asano, N.; Miyatake, K.; Uchida, H.; Watanabe, M. *J. Electrochem. Soc.* **2006**, *153*, A1154–A1158.
(10) Kreuer, K. D.; Fuchs, A.; Ise, M.; Spaeth, M.; Maier, J. *Electrochim. Acta* **1998**, *43*, 1281–1288.
(11) Munch, W.; Kreuer, K. D.; Silvestri, W.; Maier, J.; Seifert, G. *Solid State Ionics* **2001**, *145*, 437–443.
(12) Schuster, M. F. H.; Meyer, W. H.; Schuster, M.; Kreuer, K. D. *Chem. Mater.* **2004**, *16*, 329–337.
(13) Wainright, J. S.; Wang, J. T.; Weng, D.; Savinell, R. F.; Litt, M. *J. Electrochem. Soc.* **1995**, *142*, L121–L123.
(14) Wang, J. T.; Savinell, R. F.; Wainright, J.; Litt, M.; Yu, H. *Electrochim. Acta* **1996**, *41*, 193–7.
(15) Uchida, H.; Yamada, Y.; Asano, N.; Watanabe, M.; Litt, M. *Electrochemistry (Tokyo, Jpn.)* **2002**, *70*, 943–945.
(16) Kreuer, K.-D.; Paddison, S. J.; Spohr, E.; Schuster, M. *Chem. Rev.* **2004**, *104*, 4637–4678.
(17) Zhou, Z.; Liu, R.; Wang, J.; Li, S.; Liu, M.; Bredas, J.-L. *J.Phys. Chem. A* **2006**, *110*, 2322–2324.
(18) Subbaraman, R.; Ghassemi, H.; Zawodzinski, T. A., Jr *J. Am. Chem. Soc.* **2007**, *129*, 2238–2239.
(19) Zhou, Z.; Li, S.; Zhang, Y.; Liu, M.; Li, W. *J. Am. Chem. Soc.* **2005**, *127*, 10824–10825.
(20) Li, S.; Zhou, Z.; Zhang, Y.; Liu, M.; Li, W. *Chem. Mater.* **2005**, *17*, 5884–5886.
(21) Yeung, K.-S.; Farkas, M. E.; Kadow, J. F.; Meanwell, M. A. *Tetrahedron Lett.* **2005**, *46*, 3429–3432.
(22) Yin, Y.; Suto, Y.; Sakabe, T.; Chen, S.; Hayashi, S.; Mishima, T.; Yamada, O.; Tanaka, K.; Kita, H.; Okamoto, K.-I. *Macromolecules* **2006**, *39*, 1189–1198.
(23) Kreuer, K. D. *J. Membr. Sci.* **2001**, *185*, 29–39.
(24) Piroux, F.; Espuche, E.; Mercier, R. *J. Membr. Sci.* **2004**, *232*, 115–122.

MA7028055